JACS
JOURNAL OF THE AMERICAN CHEMICAL SOCIETY

Communication

pubs.acs.org/JACS

Dynamic HAADF-STEM Observation of a Single-Atom Chain as the Transient State of Gold Ultrathin Nanowire Breakdown

Lise-Marie Lacroix,*[,†] Raul Arenal,*[,‡,§] and Guillaume Viau[†]

[†]Laboratoire de Physique et Chimie des Nano-Objets, INSA, UPS, CNRS, UMR 5215, Université de Toulouse, F-31077 Toulouse, France

[‡]Laboratorio de Microscopias Avanzadas, Instituto de Nanociencia de Aragon, Universidad de Zaragoza, C/Mariano Esquillor s/n, 50018 Zaragoza, Spain

[§]Fundación ARAID, 50004 Zaragoza, Spain

Supporting Information

ABSTRACT: Ultrathin chemically grown gold nanowires undergo irremediable structural modification under external stimuli. Thanks to dynamic high-angle annular dark-field imaging, electron-beam-induced damage was followed, revealing the formation of linear chains of gold atoms as well as reactive clusters on the side, opening fascinating prospects for applications in both catalysis and electronic transport.

Metallic nanowires represent ideal objects for fundamental studies as well as potential applications in sensing,[1] catalysis, and electronic contacts.[2,3] Quantized conductance scaling as $2e^2/h$ was observed in atomic wires obtained by mechanical deformation via point contact,[4−6] breaking junction,[7] and electrochemical approaches.[8] Recently, ultrathin gold nanowires exhibiting a diameter of 1.7 nm and a micrometric length were synthesized by reduction of gold chloride salt in the presence of oleylamine.[9−12] These highly crystalline wires, grown along the ⟨111⟩ direction of the face-centered-cubit structure, open great prospects for electronic transport studies.[13,14] Their small diameters lead to quantized phenomena, while their extreme aspect ratios render physical contact by lithography feasible.[14,15] However, thin metal nanowires are prone to fragment into chain of spheres at high temperature, as described by the Plateau−Rayleigh instability.[16,17] The critical temperature at which this phenomenon occurs is strongly dependent on the wire surface energy and thus on the crystalline surface exposed and on the ligands adsorbed.[18] Other perturbations, such as an electron beam, can also induce such instability.[19] Radiolysis, due to plasmon losses, and knock-on damage, resulting from high-energy scattering, are the two most common types of primary damage that occur in irradiated samples,[20] depending on their electronic state.[21,22] We report here the first dynamic study of the breaking of a Au wire by high-angle annular dark-field scanning tunneling electron microscopy (HAADF-STEM). Sub-atomic resolution obtained with the aberration corrected microscope, combined with the high diffusion of Au, allowed us to follow the trajectory of individual atoms, evidencing the formation of atom chains prior to the breaking and free clusters on the side.

Following a previously reported method, 1.7 nm ultrathin Au nanowires were obtained in liquid phase (Figure 1a).[23] Briefly,

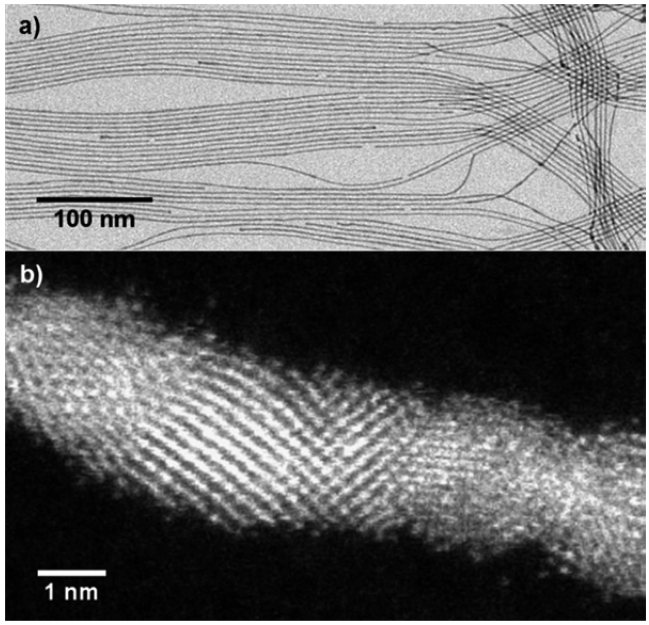

Figure 1. (a) TEM and (b) HAADF-STEM images of Au nanowires.

a 10 mM $HAuCl_4$ solution was reduced by triisopropylsilane in the presence of oleylamine at 40 °C for 1.5 h. The reducing agent and excess surfactant were removed by purification prior to the deposition of Au wires on the carbon-coated Cu grid. An electron-beam shower, lasting 20−25 min, was performed in situ to prevent contamination during STEM experiments. The HAADF-STEM study was performed with an aberration-corrected microscope working at 80−300 kV. The aberration-free probe is taken to have a 25 mrad convergent semi-angle, providing a resolution of ∼1.3 Å at 80 kV and ∼0.8 Å at 300 kV. The inner and outer collection angles used in recording the HAADF images were 60 and 200 mrad, respectively. Low

Received: July 29, 2014
Published: September 4, 2014

dx.doi.org/10.1021/ja507728j | J. Am. Chem. Soc. 2014, 136, 13075−13077

electron doses of 0.0145 $e^- A^{-2} s^{-1}$ (80 kV) and 1.1 $e^- Å^{-2} s^{-1}$ (300 kV) were employed.

The Z-contrast nature of HAADF-STEM imaging makes this method an ideal technique for identifying heavy atoms (such as gold, $Z = 79$) on light supports (such as carbon, $Z = 6$, in the present case), as evidenced in Figure 1b. Surprisingly, at 80 kV and under a very low electron dose (0.0145 $e^- A^{-2} s^{-1}$), the degradation of Au nanowires was extremely fast (Supporting Information, Videos S2 and S3). However, at 300 kV, the damage induced by the electron beam could be dynamically followed using a scanning rate of 1.6 frame·s^{-1} (Videos S4–S10). It is well established that a higher accelerating voltage reduces radiolysis damage due to the lower probability of inelastic scattering. However, the opposite happens for knock-on damage, the threshold for gold clusters and particles being above 200 and 400 kV, respectively.[24,25] As a consequence, although gold is a good conductor, the evolution of these Au nanowires seems to be governed by radiolysis at low voltage.

At 300 kV, atomic columns as well as individual atoms on the side of the wire could be detected, as evidenced in Figure 1b. The wire breaking occurred through a continual structural reorganization, with multiple twin boundaries, as well as a thickening of the initial diameter, leading to rough surfaces, as evidenced in Figure 2 and Video S3.

Contrary to the theoretical model of Plateau–Rayleigh instability,[26] the breakdown involves first an asymmetric modification of the apexes. Moreover, prior to disruption, two types of chains were observed, exhibiting thicknesses of three or four atoms (Video S4–S7 and Figure S1) or of a single atom (Video S4, S8, and S9, Figures 2a,b and S2). The single-atom chains (SACs) result from the downsizing of the channel from a diameter of three or four atoms down to a single one, as evidenced by the successive snapshots in Figure 2a,b, extracted from Video S4. In contrast, some multi-atom chains (MACs) exhibit a different behavior and break very suddenly (Figure S3). These two types of chains were previously reported for gold nanowires obtained by HRTEM irradiation of a gold polycrystalline thin film.[27] In that work, Rodrigues et al. invoked the different crystalline orientations of the atom chains obtained, [110] versus [111] or [100], respectively, to explain the discrepancy. Starting from single-crystalline Au nanowires grown along the ⟨111⟩ direction, we did not expect such variety.

Due to the constant rotation of the wire under the electron beam, the atomic positions could not always be resolved. We followed two cases of SAC and MAC breaking, for which the wire stays in zone axis. In the case of SAC formation (Figure S4), the wire remained highly crystalline along the ⟨111⟩ direction, with a continuity of the dense plane across the junction. If twin planes are mobile, as previously reported,[28,29] the apexes rotates only of few degrees (~2°) relative to each other (Figure S4). The SAC exhibits an important flexibility, as evidenced by the drastic modification of its inclination, likely due to the mobility of the anchoring atoms.[30] The interatomic distance within atom chains was found to be in the range of 0.23–0.31 nm, with a median at 0.29 ± 0.10 nm, in agreement with the nearest-neighbor distance in gold (0.29 nm).[30] The larger interatomic distance of 0.31 nm may result from carbon contamination, as previously reported.[31] In the case of MAC formation (Figure S5), important recrystallization occurred. In contrast to the SAC, in the MAC the dense planes are highly tilted, resulting in apex rotation of 23° relative to the ⟨111⟩ direction. The position of atoms in the MAC was analyzed and

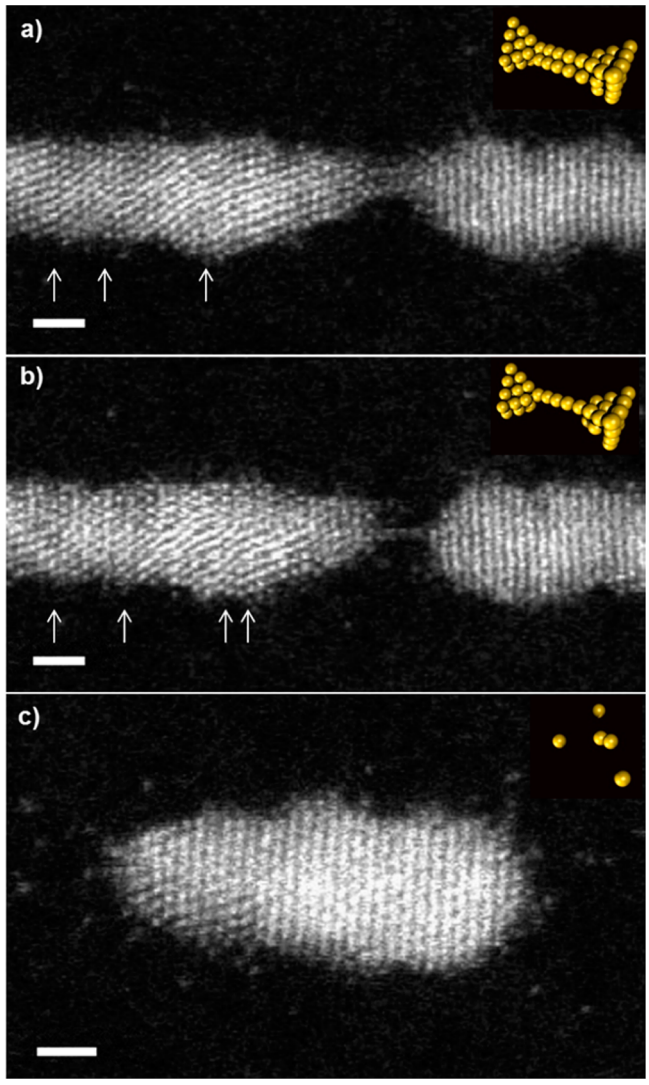

Figure 2. Snapshots extracted from Video S4 of electron-beam-induced wire breaking which proceeds through the decrease of the channel diameter from (a) three atoms to (b) a single atom. (c) The resulting 7 nm rods surrounded by Au atoms and dimers. Insets: schematic 3D views of (a) multi-atom-thick chains, (b) single-atom-thick chains, and (c) dimer and isolated atoms. Scale bar = 1 nm. White arrows indicate twin planes.

revealed unambiguously a portion of the dense plane (60° angles) with slight positional disorder (Figure S5). The interatomic distance was found to be in the range of 0.24–0.29 nm. Contrary to the previous reports, the observed MAC is only one atom thick and does not exhibit helical multi-shell structure.[32]

Concomitant with the chain formation, individual Au atoms were steadily ejected and migrated from the shrinking channel. The trajectory of each atom could be followed, evidencing the formation of small clusters such as dimers or trimers. These clusters were fairly unstable and could dissociate after a few seconds to yield isolated atoms. Such metallic clusters have been reported to be highly reactive for catalysis—in the case of gold, toward CO oxidation.[33,34] Combined with the presence of the highly twinned and rough Au wires,[35] enhanced catalytic activities are expected.

Formation of a quantized atomic channel along the wire length is clearly evidenced during the fragmentation process.

dx.doi.org/10.1021/ja507728j | J. Am. Chem. Soc. 2014, 136, 13075–13077

These intermediate states were stable enough to be imaged at 300 kV for a few seconds. Modification of the wire surface energy, through ligand-exchange processes, could make it possible to further stabilize the single-atom-thick chains,[8,36] and thus open great prospects for the easily-made parallel quantized wires. The appearance of small and highly reactive clusters strengthens the potential of ultrathin Au nanowires for catalysis. Though our study was conducted under electron beam irradiation, similar breaking mechanisms, involving channel shrinking and ejection of reactive atoms, may occur under other external stimuli such as increasing current flow or temperature, commonly used for Rayleigh instability studies.

■ ASSOCIATED CONTENT

Supporting Information

Experimental details and Videos S2−S10 (file names si_002.avi to si_010.avi). This material is available free of charge via the Internet at http://pubs.acs.org.

■ AUTHOR INFORMATION

Corresponding Authors

lmlacroi@insa-toulouse.fr
arenal@unizar.es

Notes

The authors declare no competing financial interest.

■ ACKNOWLEDGMENTS

The authors acknowledge financial support from the Labex NEXT, No. 11 LABX 075, and the European Associated Laboratory LEA TALEM. The scanning transmission electron microscopy studies were conducted at the Laboratorio de Microscopias Avanzadas at the Instituto de Nanociencia de Aragon, Universidad de Zaragoza. The transmission electron microscopy measurements were supported by the European Union Seventh Framework Program under Grant Agreement 312483-ESTEEM2 (Integrated Infrastructure Initiative−I3).

■ REFERENCES

(1) Kisner, A.; Heggen, M.; Mayer, D.; Simon, U.; Offenhäusser, A.; Mourzina, Y. *Nanoscale* **2014**, *6*, 5146.
(2) Pud, S.; Kisner, A.; Heggen, M.; Belaineh, D.; Temirov, R.; Simon, U.; Offenhäusser, A.; Mourzina, Y.; Vitusevich, S. *Small* **2013**, *9*, 846.
(3) Loubat, A.; Escoffier, W.; Lacroix, L.-M.; Viau, G.; Tan, R.; Carrey, J.; Warot-Fonrose, B.; Raquet, B. *Nano Res.* **2013**, *6*, 644.
(4) Lagos, M. J.; Sato, F.; Autreto, P. A. S.; Galvão, D. S.; Rodrigues, V.; Ugarte, D. *Nanotechnology* **2010**, *21*, 485702.
(5) Olesen, L.; Laegsgaard, E.; Stensgaard, I.; Besenbacher, F.; Schiotz, J.; Stoltze, P.; Jacobsen, K. W.; Norskov, J. K. *Phys. Rev. Lett.* **1994**, *72*, 2251.
(6) Ohnishi, H.; Kondo, Y.; Takayanagi, K. *Nature* **1998**, *395*, 780.
(7) Yanson, A. I.; Bollinger, G. R.; Van den Brom, H. E.; Agrait, N.; Van Ruitenbeek, J. M. *Nature* **1998**, *395*, 783.
(8) Leroux, Y. R.; Fave, C.; Zigah, D.; Trippe-Allard, G.; Lacroix, J. C. *J. Am. Chem. Soc.* **2008**, *130*, 13465.
(9) Halder, A.; Ravishankar, N. *Adv. Mater.* **2007**, *19*, 1854.
(10) Feng, H.; Yang, Y.; You, Y.; Li, G.; Guo, J.; Yu, T.; Shen, Z.; Wu, T.; Xing, B. *Chem. Commun.* **2009**, 1984.
(11) Kang, Y.; Ye, X.; Murray, C. B. *Angew. Chem., Int. Ed.* **2010**, *49*, 6156.
(12) Pazos-Pérez, N.; Baranov, D.; Irsen, S.; Hilgendorff, M.; Liz-Marzán, L. M.; Giersig, M. *Langmuir* **2008**, *24*, 9855.
(13) Roy, A.; Pandey, T.; Ravishankar, N.; Singh, A. K. *AIP Adv.* **2013**, *3*, 032131.
(14) Chandni, U.; Kundu, P.; Kundu, S.; Ravishankar, N.; Ghosh, A. *Adv. Mater.* **2013**, *25*, 2486.
(15) Chandni, U.; Kundu, P.; Singh, A. K.; Ravishankar, N.; Ghosh, A. *ACS Nano* **2011**, *5*, 8398.
(16) Karim, S.; Toimil-Molares, M. E.; Ensinger, W.; Balogh, A. G.; Cornelius, T. W.; Khan, E. U.; Neumann, R. *J. Phys. Appl. Phys.* **2007**, *40*, 3767.
(17) Karim, S.; Toimil-Molares, M. E.; Balogh, A. G.; Ensinger, W.; Cornelius, T. W.; Khan, E. U.; Neumann, R. *Nanotechnology* **2006**, *17*, 5954.
(18) Ciuculescu, D.; Dumestre, F.; Comesaña-Hermo, M.; Chaudret, B.; Spasova, M.; Farle, M.; Amiens, C. *Chem. Mater.* **2009**, *21*, 3987.
(19) Kura, H.; Ogawa, T. *J. Appl. Phys.* **2010**, *107*, 074310.
(20) Marks, L. D. *Rep. Prog. Phys.* **1994**, *57*, 603.
(21) Arenal, R.; Lopez-Bezanilla, A. *ACS Nano* **2014**, *8*, 8419.
(22) *In-situ Electron Microscopy at High Resolution*; World Scientific: Singapore, 2008.
(23) Loubat, A.; Impéror-Clerc, M.; Pansu, B.; Meneau, F.; Raquet, B.; Viau, G.; Lacroix, L.-M. *Langmuir* **2014**, *30*, 4005.
(24) Wang, Z. W.; Palmer, R. E. *Nanoscale* **2012**, *4*, 4947.
(25) Smith, D. J.; Petford-Long, A. K.; Wallenberg, L. R.; Bovin, J.-O. *Science* **1986**, *233*, 872.
(26) Nichols, F. A. *J. Mater. Sci.* **1976**, *11*, 1077.
(27) Rodrigues, V.; Fuhrer, T.; Ugarte, D. *Phys. Rev. Lett.* **2000**, *85*, 4124.
(28) Roy, A.; Kundu, S.; Müller, K.; Rosenauer, A.; Singh, S.; Pant, P.; Gururajan, M. P.; Kumar, P.; Weissmüller, J.; Singh, A. K.; Ravishankar, N. *Nano Lett.* **2014**, *14*, 4859.
(29) Kundu, P.; Turner, S.; Van Aert, S.; Ravishankar, N.; Van Tendeloo, G. *ACS Nano* **2014**, *8*, 599.
(30) Rodrigues, V.; Ugarte, D. *Phys. Rev. B* **2001**, 63.
(31) Galvão, D. S.; Rodrigues, V.; Ugarte, D.; Legoas, S. B. *Mater. Res.* **2004**, *7*, 339.
(32) Kondo, Y. *Science* **2000**, *289*, 606.
(33) Corma, A.; Concepción, P.; Boronat, M.; Sabater, M. J.; Navas, J.; Yacaman, M. J.; Larios, E.; Posadas, A.; López-Quintela, M. A.; Buceta, D.; Mendoza, E.; Guilera, G.; Mayoral, A. *Nat. Chem.* **2013**, *5*, 775.
(34) Zhou, M.; Zhang, A.; Dai, Z.; Zhang, C.; Feng, Y. P. *J. Chem. Phys.* **2010**, *132*, 194704.
(35) Rashkeev, S.; Lupini, A.; Overbury, S.; Pennycook, S.; Pantelides, S. *Phys. Rev. B* **2007**, 76.
(36) Huisman, E. H.; Trouwborst, M. L.; Bakker, F. L.; de Boer, B.; van Wees, B. J.; van der Molen, S. J. *Nano Lett.* **2008**, *8*, 3381.